

## Article

# A Study on Fishing Vessel Energy System Optimization Using Bond Graphs

Sang-Won Moon <sup>1</sup>, Won-Sun Ruy <sup>2,\*</sup>  and Kwang-Phil Park <sup>2</sup>

<sup>1</sup> Fishing Vessel Safety Policy Division & Fisheries Policy Division, Ministry of Oceans and Fisheries, Sejong 30110, Republic of Korea; swmoon7@korea.kr

<sup>2</sup> Department of Autonomous Vehicle System Engineering, Chungnam National University, Deajeon 34134, Republic of Korea; kppark@cnu.ac.kr

\* Correspondence: wsruy@cnu.ac.kr; Tel.: +82-42-821-6623; Fax: +82-42-823-5437

**Abstract:** Recently, environmental regulations have been strengthened due to climate change. This change comes in a way that limits emissions from ships in the shipbuilding industry. According to these changes, the trend of ship construction is changing installing pollutant emission reduction facilities such as scrubbers or applying alternative fuels such as low sulfur oil and LNG to satisfy rule requirements. However, these changes are focused on large ships. Small ships are limited in size. So, it is hard to install large facilities such as scrubbers and LNG propulsion systems, such as fishing boats that require operating space. In addition, in order to apply the pure electric propulsion method, there is a risk of marine distress during battery discharge. Therefore, the application of the electric–diesel hybrid propulsion method for small ships is being studied as a compromised solution. Since hybrid propulsion uses various energy sources, a method that can estimate effective efficiency is required for efficient operation. Therefore, in this study, a Bond graph is used to model the various energy sources of hybrid propulsion ships in an integrated manner. Furthermore, based on energy system modeling using the Bond graph, the study aims to propose a method for finding the optimal operational scenarios and reduction ratios for the entire voyage, considering the navigation feature of each different maritime region. In particular, the reduction gear is an important component at the junction of the power transmission of the hybrid propulsion ship. It is expected to be useful in the initial design stage as it can change the efficient operation performance with minimum design change.

**Keywords:** bond graph; hybrid propulsion; ship efficiency; energy system modeling; green ship



**Citation:** Moon, S.-W.; Ruy, W.-S.; Park, K.-P. A Study on Fishing Vessel Energy System Optimization Using Bond Graphs. *J. Mar. Sci. Eng.* **2024**, *12*, 903. <https://doi.org/10.3390/jmse12060903>

Academic Editor: Rosemary Norman

Received: 8 May 2024

Revised: 24 May 2024

Accepted: 25 May 2024

Published: 28 May 2024



**Copyright:** © 2024 by the authors. Licensee MDPI, Basel, Switzerland. This article is an open access article distributed under the terms and conditions of the Creative Commons Attribution (CC BY) license (<https://creativecommons.org/licenses/by/4.0/>).

## 1. Introduction

Recently, environmental regulations, such as carbon neutrality, are on the rise due to climate change, and this trend is also applied to shipping industry [1]. As a result, regulations and rules governing ship emissions, ranging from  $\text{NO}_x$  and  $\text{SO}_x$  to  $\text{CO}_2$ , are being strengthened or newly established, primarily under the auspices of the Marine Environment Protection Committee (MEPC) of the International Maritime Organization (IMO). In response to these demands of the times, the construction trend of ships is changing with a propulsion method using eco-friendly fuels. Looking at the trend, it was initially shown that facilities such as scrubbers were added to existing ships to satisfy the rule and regulation on  $\text{SO}_x$  emission restrictions, etc., to install engines applied with low sulfur oil on new ships [2,3]. In addition, it has been expanded from using BOG (boil-off gas) of LNG carriers as propulsion fuel to pure LNG propulsion ships [4,5]. Recently, research on discovering new fuels such as LPG, DME, and ammonia and applying them to ships has been actively conducted [6–8].

However, this transition to eco-friendly ships is concentrated on medium and large-sized ships. The constraint in the transition of small ships to eco-friendly ships is due to the weak R&D base of small shipyards, but the main reason is the small size of the ship.

Compared to the existing heavy fuel oil (Bunker C oil), the size of the fuel tank is bound to increase because the energy density per volume is small. Therefore, there is a limit to the application of small ships with space restrictions [9]. In particular, the majority of the Republic of South Korea's 72,000 vessels, with most being fishing vessels (around 64,000), are subject to legal size restrictions aimed at preventing the overexploitation of marine resources [10,11]. Among them, coastal fishing boats (about 61,000 vessels) cannot be built in excess of 10 tons (tonnage) [12,13]. Additionally, fishing vessels, unlike cargo ships, require operational spaces for lowering and retrieving nets, and treating and sorting fish at sea. In other words, considering the ship owner's demand to have as wide a workspace as possible for fishing on the main deck, designs such as installing LNG tanks on deck are less field-soluble. In addition to the size restrictions and the necessity for operational space for fishing operations, small fishing vessels have distinctive features that contrast with large ships. In accordance with fishing methods, there are around 40 different types of vessels, each customized to the characteristics of the East, West, and South Sea areas surrounding the Republic of Korean Peninsula. As a result, the owner's needs for ship design also vary to consider target fish, which act as constraints during construction. Additionally, despite occupying a significant portion of Korea's domestic shipbuilding industry due to its strong domestic market, such as the construction of more than 2000 new ships per year, it is challenging to conduct research and development independently because most of them are built in small shipyards. It is challenging to acquire the same fundamental technology as an eco-friendly ship because these small shipyards are designed in a way that slightly modifies their existing designs.

In such circumstances, considering electric propulsion methods for small fishing vessels could be an option for transitioning to green ships [14]. However, considering that electric power consumption to operate facilities such as fishing gear takes one to two days per navigation, there is a risk of distress when the battery runs out, so there is a limit to the application. Therefore, as a national study in the Republic of Korea, research is being conducted to apply a hybrid propulsion method in which electric batteries are applied to existing diesel engines for small fishing vessels that are less than 10 tons [15].

As the hybrid propulsion method is applied, the propulsion system becomes more complex and creates another design problem. Previously, the design was carried out by estimating the main engine according to ship resistance on design speed, but when the hybrid propulsion method is applied, a new question arises as to what mode should be applied for each operation scenario to consider the entire navigation. For example, when moving to the port and the operating site, the target ship speed is different, and at this time, it is necessary to decide which of the hybrid propulsion methods to adopt. Hybrid propulsion in the automotive industry, now widely adopted, also distinguishes itself. Unlike cars, which typically find it difficult to determine fixed routes and target speeds, ships operate with defined routes and target speeds. To solve this problem, it can be used as a basis for determining the decision by measuring the efficiency for each mode of operation scenario. Currently, there are methods such as the Energy Efficiency Existing Ship Index (EEDI), which is the ratio for CO<sub>2</sub> emissions to a ship's transport capacity, to assess efficiency [16]. In addition, the efficiency of the ship can be reviewed as the ratio of effective power to indicated power, but it is difficult to calculate the hybrid power conversion process incorporating various energy sources. Therefore, it is necessary to consider a methodology that can comprehensively model a hybrid propulsion method with various energy sources and effectively analyze energy flow. In a previous study, changes in voltage and power were analyzed using a Bond graph in a ship propulsion system where a generator engine and a battery are connected by a single motor [17,18]. Previous research is actually a study on ships using only electricity as an energy source, which is different from the subject of this study on ships propelled by diesel engines and motors connected to electric batteries. In summary, there are not many studies that apply the Bond graph to ship propulsion systems, and similar prior studies are difficult to apply to hybrid

propulsion ships with diesel engines and electric batteries, and there is no approach to efficiency estimation.

However, the Bond graph method used in previous studies can model targets in various areas such as machinery, electricity, and hydraulic pressure, effectively modeling the energy system of ships propelled by motors through electric batteries and diesel engines [19]. In addition, Bond graphs have the advantage of efficiently analyzing complex subjects by connecting each element to power, allowing for the calculation of energy flow, while also enabling the understanding of physical connection structures similar to the block diagram. In other words, since the Bond graph enables computational modeling and physical modeling at the same time, it can be used to analyze objects and, conversely, can be used as a means of optimization.

Therefore, in this study, a Bond graph was used to model the energy system for the propulsion system of a 9.77 tons hybrid propulsion (diesel engine + electric motor) coastal gill net fishing vessel. We try to judge the usefulness with a methodology that can analyze energy flow. Furthermore, the aim of the research extends beyond previous studies to establish a foundation for identifying the optimal operation mode of each hybrid propulsion system, and to select the optimal equipment specifications for this purpose. For reference, information related to the 9.77-ton coastal gill net vessel and relevant fishing regulations can be verified by searching on the National Institute of Fisheries Science website [20]. The general main specifications are shown in Table 1. Additionally, additional information on fishing vessels can be checked through the “Illustrations of Korean Fishing Vessels (2018)” published by the National Institute of Fisheries Science [21]. Previous research has focused on the performance evaluation of ships with a single energy source. In contrast, this study presents optimal operational power and equipment specifications for ships applying various energy sources. This is a key difference. In summary for this study, ships follow set navigation patterns, and the entire voyage can be divided into multiple navigation scenarios. When a hybrid propulsion system is applied, appropriate navigation modes and optimal power must be determined for each scenario. Additionally, suitable equipment capable of achieving these performances must be selected. This is illustrated in Figure 1.

**Table 1.** Normal principal dimension of 9.77 ton coastal gill net fishing vessel.

Tonnage	Length (m)	Breadth (m)	Depth (m)	Knots
9.77	11.5~17.46	2.52~4.52	0.79~1.66	10~12

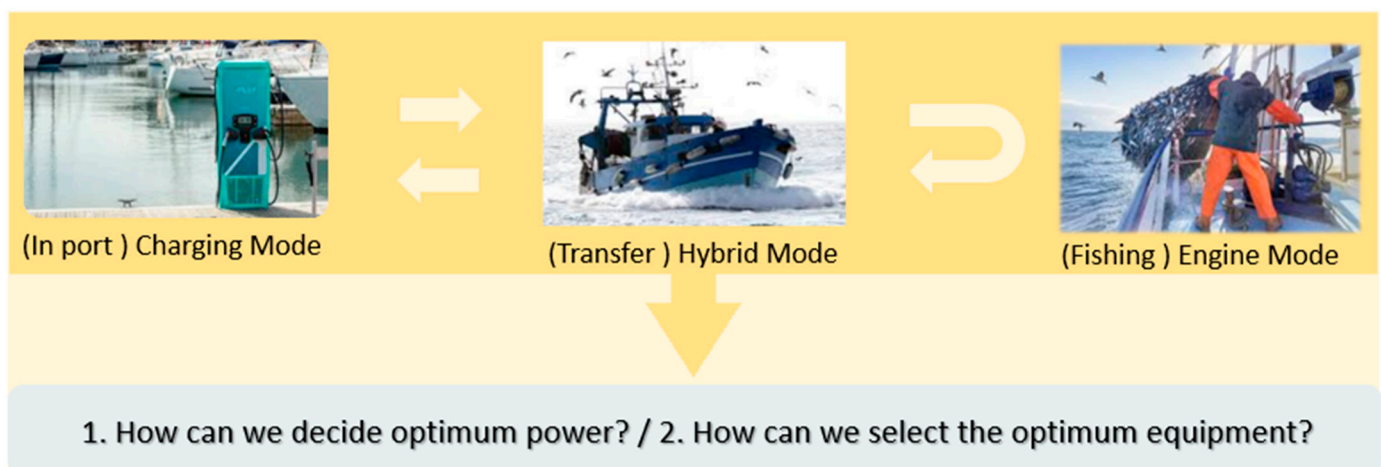


**Figure 1.** Concept of problem.

## 2. Fundamental of Bond Graph

### 2.1. Overview of Bond Graph

The Bond graph is a method proposed by Prof. Paynter in 1959 to structure each element of the analysis by connecting it with power [22]. It has started and developed by defining power exchange and energy flow between each element as a Bond graph methodology.

The core principle of the Bond graph can be said to be energy conversion based on the conservation law. Since energy is only transformed and preserved in shape, the Bond graph can be expressed in an integrated way for various domains such as machinery, electricity, heat, and fluid power. Therefore, it can be said that the Bond graph presents a method of effectively dealing with energy conversion based on a unified notation. In order to effectively understand the Bond graph based on these core principles, it is necessary to understand the variables, elements, causality between variables, and notation that make up the Bond graph [23,24].

### 2.2. Variable of Bond Graph

Variables in the Bond graph are categorized into power variables and energy variables. Power variables are again distinguished into effort ( $e$ ) and flow ( $f$ ), while energy variables are divided as momentum ( $p$ ) and displacement ( $q$ ). A power variable is a constituent variable of a bond that connects each element. All elements are connected by a bond, and the bond consists of effort ( $e$ ) and flow ( $f$ ). Power is defined as the product of effort ( $e$ ) and flow ( $f$ ) [power = effort ( $e$ )  $\times$  flow ( $f$ )]. The reason why the variables are newly defined as effort ( $e$ ) and flow ( $f$ ) in the Bond graph is to unify and distinguish the variables that make up power for objects in various domains into effort ( $e$ ) and flow ( $f$ ). As some examples, variables for each domain are divided into effort ( $e$ ) and flow ( $f$ ) as shown in the following Table 2.

**Table 2.** Power variable and energy variables of various domains.

Description	Domain	Effort ( $e$ )	Flow ( $f$ )
Power variable	Mechanics translational	Force $F$ [N]	Velocity $v$ [m/s]
	Mechanics rotational	Angular moment $M$ [N·m]	Angular velocity $\omega$ [rad/s]
	Electronics	Voltage $u$ [V]	Current $i$ [A]
	Hydraulic	Pressure $P$ [N/m <sup>2</sup> ]	Volume flow $Q$ [m <sup>3</sup> /s]
Energy variable	Mechanics translational	Momentum $P$ [N·s]	Displacement $x$ [m]
	Mechanics rotational	Angular Momentum $p\omega$ [N·ms]	Angle $\theta$ [rad]
	Electronics	Linkage flux $\lambda$ [V·s]	Charge $q$ [A·s]
	Hydraulic	Pressure Momentum $p_p$ [N/m <sup>2</sup> s]	Volume $V$ [m <sup>3</sup> ]

The reason for distinguishing energy variables is momentum ( $p$ ) and displacement ( $q$ ) is for conversion between effort ( $e$ ) and flow ( $f$ ) in the Bond graph. After modeling with the Bond graph, effort ( $e$ ) and flow ( $f$ ) values in all connections (bonds) should be computed. At this time, the value regarding the specification of each element of effort ( $e$ ) and flow ( $f$ ) becomes known, while the energy storage element becomes unknown as a variable because it changes with time. Therefore, it is necessary to find the unknown term through the known term, and in this process, the conversion between effort ( $e$ ) and flow ( $f$ ) is required. Variables used in this transformation process are energy variables namely momentum ( $p$ ) and displacement ( $q$ ). Each definition is as below in Table 3, and a detailed transformation process will be described in causality between variables.

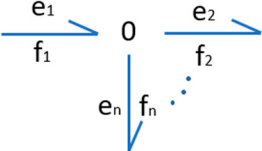
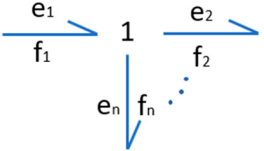
**Table 3.** Generalized momentum ( $p$ ) and displacement ( $q$ ).

Generalized Momentum ( $p$ )	Generalized Displacement ( $q$ )
$p(t) = p(t)_0 + \int_0^t e(t)dt$	$q(t) = q(t)_0 + \int_0^t f(t)dt$

2.3. Element of Bond Graph

In the Bond graph, elements are divided into sources, storage, transform, converter, dissipator, and distribute. Examining each category is as follows. The source ( $S_e$ ) is an element that supplies power to the entire system and includes, for example, engine torque and battery current. Storage ( $I$ ) is an element that stores power and includes inertia, which stores rotational inertia, and capacity for electric power. Transform ( $TF$ ) is an element that transforms effort to effort or flow to flow in a constant ratio, and a representative example is gear. The changes in Effort ( $e$ ) and Flow ( $f$ ) by Transform ( $TF$ ) are shown in Table 4. Convert ( $GY$ ) is an element that converts between effort to flow or flow to effort at a certain ratio. If motor is idealized, it can be said that this is the case. The change effort ( $e$ ) and flow ( $f$ ) by converter ( $GY$ ) is defined as Table 4. Dissipator ( $R$ ) is a resistive element that causes energy loss in the entire system. Typical examples are electrical resistance or friction loss. Distribute is an element that connects previous elements and distributes power. It is classified into 0 Junction and 1 Junction, and all elements connected to 0 Junction have the same effort, and all elements connected to 1 Junction have the same flow.

Table 4. Transform, convert and junction.

Transform	Convert
$e_1 = TF \times e_2, f_2 = TF \times f_1$	$e_1 = GY \times f_2, e_2 = GY \times f_1$
0 Junction	1 Junction
<div><math display="block">e_1 = e_2 = \cdots = e_n</math><math display="block">f_1 = f_2 + \cdots + f_n</math><math display="block">f_1 - f_2 - \cdots - f_n = 0</math></div> 	<div><math display="block">f_1 = f_2 = \cdots = f_n</math><math display="block">e_1 = e_2 + \cdots + e_n</math><math display="block">e_1 - e_2 - \cdots - e_n = 0</math></div> 

2.4. Causality of Bond Graph

The transformation on the Bond graph between variables follows causality. Causality is classified into integral and differential types, and the transformation between variables is schematically expressed in Figure 2. Note that when calculating effort and flow, the integral type or differential type should be applied according to the model characteristics, but it should be applied uniformly without mixing [25].

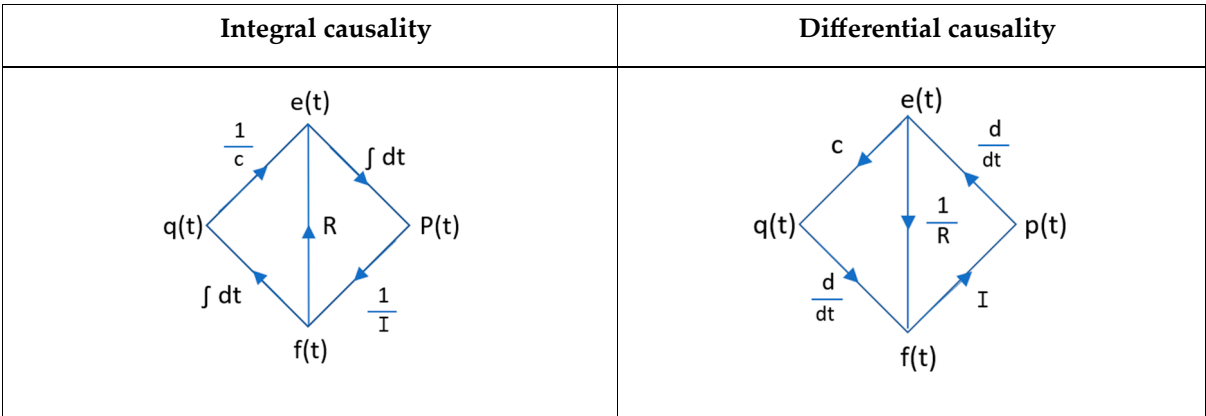


Figure 2. Integral causality vs. differential causality.

3. Analysis of the Research Vessel

3.1. Overview of the Research Vessel

The target vessels for this study are 9.77 tons of coastal gillnet fishing boats, which have the following main characteristics. Among the 72,000 vessels in the Republic of Korea,

fishing boats account for 64,000, of which 61,000 coastal fishing boats' maximum size is limited to 10 tons (tonnage) in order to protect fishery resources in accordance with the "Fisheries Act", which is the domestic law [12,13]. In other words, the target vessels in this study are small in size, but they occupy an important position as they constitute most of the ships in the Republic of Korea [10]. In addition, gill netting is a fishing method that is caught by getting entangled in a net, and facilities such as a winch (fishing gear) are required to lift the net [21]. It is generally made of FRP (fiberglass-reinforced plastic), and it takes about 1 day for one voyage with 10 to 12 knots, and the number of crew is about two to three members [21]. Currently, the development of diesel and electric complex propulsion fishing vessels is in progress to convert to eco-friendly fishing boats (Ministry of Oceans and Fisheries of the Republic of Korea (hereinafter referred to as MOF), research project on the development of energy-efficient eco-friendly fishing vessels, '21~25'). This study modeled the energy system using a Bond graph based on the fishing vessel under development.

### 3.2. Operational Scenarios of the Research Vessel

Currently, the development of diesel and electric complex propulsion fishing vessels is in progress to convert to eco-friendly fishing boats (Ministry of Oceans and Fisheries of the Republic of Korea (hereinafter referred to as MOF), research project on the development of energy-efficient eco-friendly fishing vessels, '21~25'). This study modeled the energy system using a Bond graph. In order to model the energy system of the ship to be studied, the operation scenario was analyzed based on one voyage of the ship to identify the required power. The operation scenarios per voyage can be largely categorized into in-port operation, operation when moving to the operating site, and operation on site. In addition, since fishing vessels typically do not engage in ballasting, it is assumed that it is a reverse process at the time of departure in consideration of the consumption of fuel and fresh water and increased catches at the time of return. In other words, it is assumed that there are three operation scenarios (in-port navigation, navigation when moving to fishing grounds, and navigation during fishing operations) based on the fishing vessel under development. First, in order to model the propulsion system as a Bond graph and verify the modeling results, a load for each operation scenario is required. Therefore, the design load for each operation scenario of a ship under development (MOF, energy-efficient and eco-friendly fishing vessel development research project, '21~25') is used as a value for calculation verification, and the value is shown in Table 5. In addition, the load is shown together because it must be converted into a value obtained by dividing the torque by RPS in order to be applied as a resistance factor to the Bond graph modeling.

**Table 5.** Load cases according to operation scenario.

Operation Scenario	Torque [N·m] (A)	RPS (B)	Torque/RPS (A/B)
In port	5787.6	38.88	148.87
Transfer from port to fishing ground	10,403.4	53.83	193.27
Working (fishing)	8292.99	44.86	184.88

### 3.3. Research Vessel's Propulsion Modes

The target vessel for this study is a hybrid propulsion method that is propelled by a diesel engine and electric motor supplied with power from the battery. Basically, there may be engine propulsion, electric motor propulsion, and engine–electric motor complex propulsion methods. However, if the electric motor propulsion is used only as much as the battery is charged on shore, the use time of the electric motor propulsion is limited, so it is necessary to be able to charge the battery in consideration of the power required for each operation scenario when promoting the diesel engine. Therefore, there are four mode cases

in the ship to be studied: hybrid mode, engine mode, motor mode, and charging mode which use both the engine and the motor.

### 3.4. Analysis of Research Vessel's Specifications

The ship to be studied was assumed to be based on the specifications of the diesel and electric complex propulsion fishing vessel under development (MOF, energy-efficient and eco-friendly fishing vessel development research project, '21~25'), and unconfirmed information was assumed by referring to the specifications of existing similar ships. In addition, it was assumed that the power required for the fishing gear during operation was supplied by electricity produced by a generator engine and was independent of the battery for propulsion. The variables constituting the Bond graph modeling of the propulsion system of the ship to be studied are summarized in Table 6.

**Table 6.** Equipment specification for Bond graph modeling.

Description	Mechanical	Electrical
Source (S)	$S_e$ (Engine Torque): 2461.6 [N·m]	$S_e$ (Battery Voltage): 671.6 [V]
Storage (I)	$J_F$ (Inertia of engine flywheel): 1.612 [kg·m <sup>2</sup> ] $J_R$ (Inertia of motor rotor): 0.84 [kg·m <sup>2</sup> ]	$L$ (Inductance on PTI *†): 0.000659 [H] *† Power Take In(PTI) of motor
Resister (R)	$T$ (Load according to operation scenario): Refer to "Torque/PRS" on Table 5 $\alpha$ (Load of battery charging)  : 6.516 [N·m/(rad/s)] $\beta$ (Resistance of stern tube)  : $T x 0.005$ *† [N·m/(rad/s)] *† Friction coefficient $\gamma$ (Resistance of motor bearing)   : 0.0038 [N·m/(rad/s)]	$R_E$   (Resistance of motor coil on PTI) : 0.162 [Ω] $R_C$   (Resistance of converter coil): 0.145 [Ω]
Transformer (TF)	$TF$ (Gear ratio): 1:3.5 ( $N_2 > N_1$ , $N_1 = m_1$ , $N_2 = m_2$ )	
Gyrator (GY)	$KC$ (Convertor): 3.86 *† *†   671.6 battery voltage(effort) change to 174 convertor ampere(flow) $\Rightarrow 671.6 / 174 = 3.86$	$KM$ (Motor): 3.23 *† *†   172.4 motor ampere(flow) changed to 557 motor torque(effort) $\Rightarrow 557 / 172.4 = 3.23$

## 4. Modeling Using Bond Graph

The Bond graph modeling was conducted in the flow as shown in Figure 3, and the detailed process of Bond graph modeling for the target ship is described sequentially as follows.

The propulsion system of the research vessel is described as a 3D image, the Scheme and Bond graph modeling results are described sequentially as follows. Figure 4 is the expression of the propulsion system of the research vessel as a 3D image, and it is revealed that it is only an illustration for effective explanation and not actual information used in this study.

Since it is difficult to model directly with a Bond graph in the state of Figure 4, each component from the engine and battery to propeller is converted into an element for Bond graph modeling, and the scheme is created in Figure 5 [26].

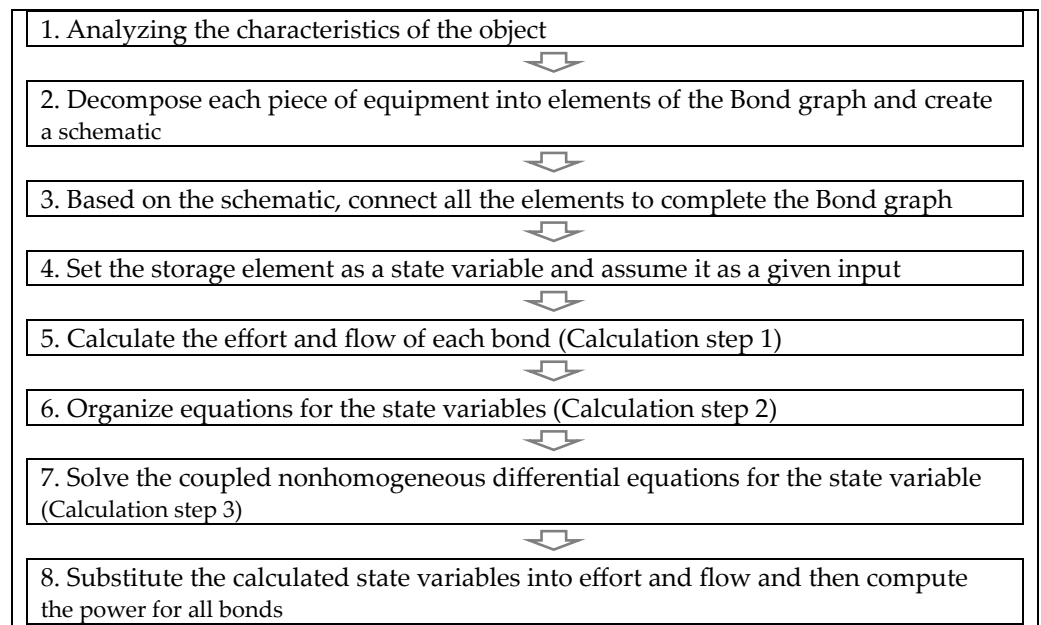


Figure 3. Bond graph modeling flow chart.

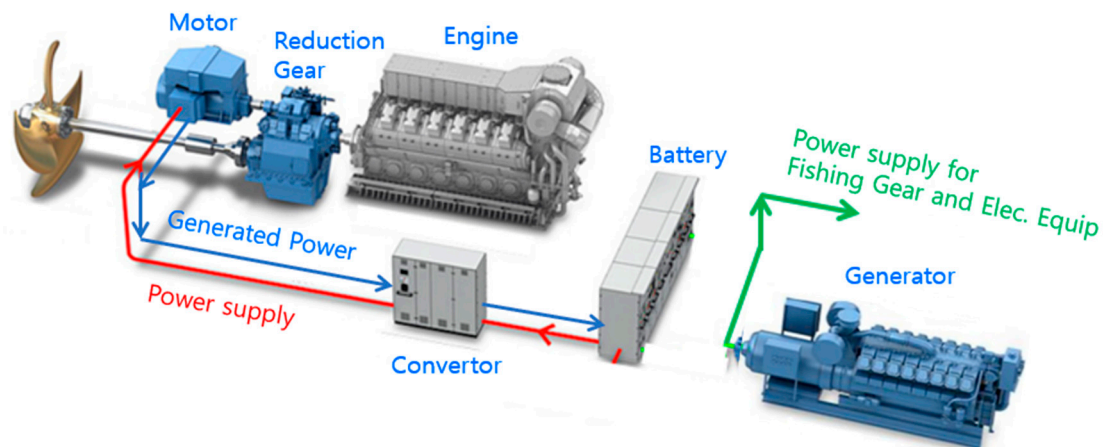


Figure 4. Three-dimensional modeling of energy system.

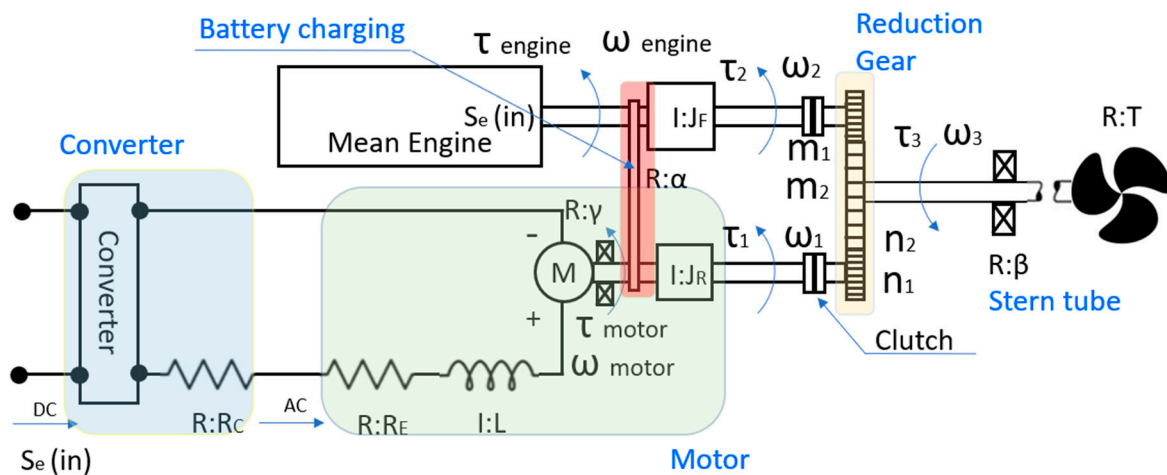
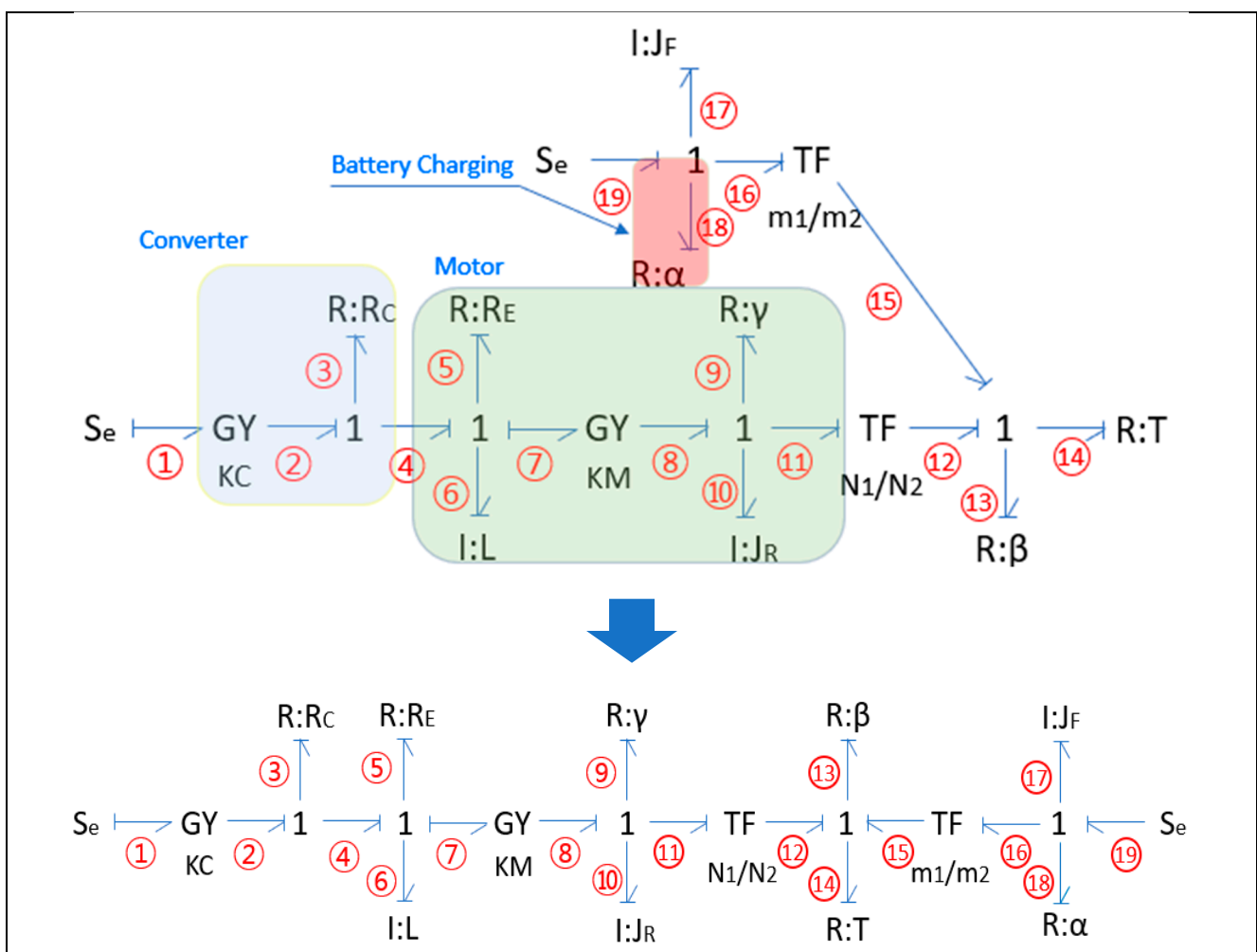


Figure 5. Scheme of energy system for Bond graph modeling.

Based on the above scheme, if the propulsion system of the target vessel for this study is idealized with a Bond graph, the following results are obtained [27].

### 5. Energy Flow Calculation

As depicted in Figure 6, the propulsion system of the research vessel was modeled using a Bond graph. Next, the effort and flow of each bond in the model represented in Figure 6 will be calculated to understand the energy variations. In this process, it is crucial to set the energy variable of the storage element as a state variable, assuming the unknowns as known variables. Subsequently, organizing equations for the state variables leads to a system of ordinary differential equations. By assigning initial values and solving, the effort and flow for all bonds can be obtained. Calculations for the most complex hybrid mode of the research vessel are presented below. The subscript numbers in the following calculation represent the respective bond numbers. Sequential calculations from bond 1 to 19 are as follows.



**Figure 6.** Bond graph modeling of energy system.

As shown in Figure 6, the propulsion system of the ship to be studied was modeled as a Bond graph. Next, the effort and flow of each bond according to the modeling of Figure 6 are calculated so that energy changes can be identified. The most important thing in this process is to assume that the unknown term is known by setting the energy variable of the storage element as a state variable. After that, if the equation for the state variable is summarized, it results in a simultaneous ordinary differential equation. At this time, if the initial value is substituted to obtain the solution, the effort and flow for all bonds can be

obtained. The calculation for the most complex hybrid mode among the operation modes of the research vessel is as follows. In the calculation process below, the subscript number represent the respective bond numbers. Sequential calculations from bond 1 to 19 are as follows.

<Calculation for Bond graph modeling—Step1.>

$$e_1 = Se_{(Battery)} \\ f_1 : e_2 = KC \times f_1, f_1 = \frac{e_2}{KC} = \frac{1}{KC} \left( R_C \times \frac{p_6}{L} + R_E \times \frac{p_6}{L} + \dot{p}_6 + KM \times \frac{p_{10}}{J_R} \right) \quad (1)$$

$$e_2 = e_3 + e_4 = R_C \times \frac{p_6}{L} + R_E \times \frac{p_6}{L} + \dot{p}_6 + KM \times \frac{p_{10}}{J_R} \\ f_2 = \frac{p_6}{L} (\because f_2 = f_3 = f_4 = f_5 = f_6 = f_7), f_2 = \frac{e_1}{KC} = \frac{Se_{(Battery)}}{KC} (\because e_1 = KC \times f_2) \quad (2)$$

$$e_3 = R \times f_3 = R_C \times \frac{p_6}{L} \\ f_3 = \frac{p_6}{L} = \frac{Se_{(Battery)}}{KC} \quad (3)$$

$$e_4 = e_5 + e_6 + e_7 = R_C \times \frac{p_6}{L} + \dot{p}_6 + KM \times \frac{p_{10}}{J_R} \\ f_4 = \frac{p_6}{L} = \frac{Se_{(Battery)}}{KC} \quad (4)$$

$$e_5 = R \times f_5 = R_E \times \frac{p_6}{L} \\ f_5 = \frac{p_6}{L} = \frac{Se_{(Battery)}}{KC} \quad (5)$$

$$e_6 = \dot{p}_6 \\ f_6 = \frac{p_6}{I} = \frac{p_6}{L} = \frac{Se_{(Battery)}}{KC} \quad (6)$$

$$e_7 = KM \times f_8 = KM \times \frac{p_{10}}{J_R} \\ f_7 = \frac{p_6}{L} = \frac{Se_{(Battery)}}{KC} \quad (7)$$

$$e_8 = KM \times f_7 = KM \times \frac{p_6}{L} \\ f_8 = \frac{p_{10}}{J_R} (\because f_8 = f_9 = f_{10} = f_{11}) \quad (8)$$

$$e_9 = R \times f_9 = \gamma \times \frac{p_{10}}{J_R} \\ f_9 = \frac{p_{10}}{J_R} \quad (9)$$

$$e_{10} = \dot{p}_{10} \\ f_{10} = \frac{p_{10}}{I} = \frac{p_{10}}{J_R} \quad (10)$$

$$e_{11} : e_8 = e_9 + e_{10} + e_{11}, e_{11} = e_8 - e_9 - e_{10} = KM \times \frac{p_6}{L} - \gamma \times \frac{p_{10}}{J_R} - \dot{p}_{10} \\ f_{11} = \frac{p_{10}}{J_R} \quad (11)$$

$$e_{12} = \frac{N_2}{N_1} \times e_{11} = \frac{N_2}{N_1} \left( KM \times \frac{p_6}{L} - \gamma \times \frac{p_{10}}{J_R} - \dot{p}_{10} \right) \\ f_{12} = \frac{N_1}{N_2} \times f_{11} = \frac{N_1}{N_2} \frac{p_{10}}{J_R} (\because f_{12} = f_{13} = f_{14} = f_{15}) \quad (12)$$

※ Reduction Gear ratio

$$N_2 > N_1 (N_1 = m_1, N_2 = m_2) \\ N_2 \times e_{11} = N_1 \times e_{12} \rightarrow e_{12} = \frac{N_2}{N_1} \times e_{11} / \quad N_1 \times f_{11} = N_2 \times f_{12} \rightarrow f_{12} = \frac{N_1}{N_2} \times f_{11}$$

$$e_{13} = R \times f_{13} = \beta \frac{N_1}{N_2} \frac{p_{10}}{J_R} \\ f_{13} = \frac{N_1}{N_2} \frac{p_{10}}{J_R} = \frac{m_1}{m_2} \frac{p_{17}}{J_F} \quad (13)$$

$$e_{14} = R \times f_{14} = T \frac{N_1}{N_2} \frac{p_{10}}{J_R} \\ f_{14} = \frac{N_1}{N_2} \frac{p_{10}}{J_R} = \frac{m_1}{m_2} \frac{p_{17}}{J_F} \left( \rightarrow \frac{p_{10}}{J_R} = \frac{p_{17}}{J_F} \right) \quad (14)$$

$$e_{19} = Se_{(Engine)} \\ f_{19} = \frac{p_{17}}{J_F} (\because f_{16} = f_{17} = f_{18} = f_{19}) \quad (15)$$

$$\begin{aligned} e_{18} &= R \times f_{18} = \alpha \frac{N_1}{N_2} \frac{p_{17}}{J_F} \\ f_{18} &= \frac{p_{17}}{J_F} \quad (\text{used to charging mode only}) \end{aligned} \quad (16)$$

$$\begin{aligned} e_{17} &= \dot{p}_{17} \\ f_{17} &= \frac{p_{17}}{I} = \frac{p_{17}}{J_F} \end{aligned} \quad (17)$$

$$\begin{aligned} e_{16} : e_{19} &= e_{17} + e_{16}, e_{16} = e_{19} - e_{17} = Se_{(Engine)} - \dot{p}_{17} \\ f_{16} &= \frac{p_{10}}{J_R} \end{aligned} \quad (18)$$

$$\begin{aligned} e_{15} &= \frac{m_2}{m_1} \times e_{16} = \frac{m_2}{m_1} (Se_{(Engine)} - \dot{p}_{17}) \\ f_{15} &= \frac{m_1}{m_2} f_{16} = \frac{m_1}{m_2} \frac{p_{17}}{J_F} \\ e_{12} + e_{15} &= e_{13} + e_{14} \\ \frac{N_2}{N_1} \left( KM \times \frac{p_6}{L} - \gamma \times \frac{p_{10}}{J_R} - \dot{p}_{10} \right) + \frac{m_2}{m_1} (Se_{(Engine)} - \dot{p}_{17}) &= \beta \frac{N_1}{N_2} \frac{p_{10}}{J_R} + T \frac{N_1}{N_2} \frac{p_{10}}{J_R} \end{aligned} \quad (19)$$

Based on the effort and flow calculations of each bond [Equations (1)~(19)], the equations for the state variables are summarized [Equation (22)], ultimately leading to the derivation of a matrix form system of coupled differential-algebraic equations [Equation (23)]. The relationship equation between the state variables  $p_{10}$  and  $p_{17}$  is derived using Equation (19). After that, rearranging Equation (20) with respect to  $p_{10}$  and similarly rearranging with respect to  $p_{17}$  results in the following.

<Calculation for Bond graph modeling—Step2.>

$$\begin{aligned} e_{12} + e_{15} &= e_{13} + e_{14} \\ \frac{N_2}{N_1} \left( KM \times \frac{p_6}{L} - \gamma \times \frac{p_{10}}{J_R} - \dot{p}_{10} \right) + \frac{N_2}{N_1} (Se_{(Engine)} - \dot{p}_{17}) &= \beta \frac{N_1}{N_2} \frac{p_{10}}{J_R} + T \frac{N_1}{N_2} \frac{p_{10}}{J_R} \quad (\because N_1 = m_1, N_2 = m_2) \end{aligned} \quad (20)$$

$$\begin{aligned} \dot{p}_{10} &= \left( \frac{1}{1+J_F/J_R} \right) \frac{KM}{KC} Se_{(Battery)} \\ &- \left( \frac{1}{1+J_F/J_R} \right) \frac{1}{J_R} \left[ \gamma + (\beta + T) \left( \frac{N_1}{N_2} \right)^2 \right] p_{10} + \left( \frac{1}{1+J_F/J_R} \right) Se_{(Engine)} \end{aligned} \quad (21)$$

$$\begin{aligned} \dot{p}_{17} &= \left( \frac{1}{J_R/J_F+1} \right) \frac{KM}{KC} Se_{(Battery)} \\ &- \left( \frac{1}{J_R/J_F+1} \right) \frac{1}{J_R} \left[ \gamma + (\beta + T) \left( \frac{N_1}{N_2} \right)^2 \right] p_{10} + \left( \frac{1}{J_R/J_F+1} \right) Se_{(Engine)} \end{aligned} \quad (22)$$

Equations (21) and (22) can be expressed as a coupled ordinary differential equation in matrix form, as follows:

<Calculation for Bond graph modeling—Step3.>

$$\begin{bmatrix} \dot{p}_{10} \\ \dot{p}_{17} \end{bmatrix} = \begin{bmatrix} \frac{-1}{(1+J_F/J_R)J_R} \left[ \gamma + (\beta + T) \left( \frac{N_1}{N_2} \right)^2 \right] & 0 \\ \frac{-1}{(J_R/J_F+1)J_R} \left[ \gamma + (\beta + T) \left( \frac{N_1}{N_2} \right)^2 \right] & 0 \end{bmatrix} \begin{bmatrix} p_{10} \\ p_{17} \end{bmatrix} + \begin{bmatrix} \frac{1}{(1+J_F/J_R)} \frac{KM}{KC} & \frac{1}{(1+J_F/J_R)} \\ \frac{1}{(J_R/J_F+1)} \frac{KM}{KC} & \frac{1}{(J_R/J_F+1)} \end{bmatrix} \begin{bmatrix} Se_{(Battery)} \\ Se_{(Engine)} \end{bmatrix} \quad (23)$$

Since the initial condition of the engine and motor is in a stationary state, if the coupled ordinary differential equations are solved by setting the initial value to 0 for time, the solution becomes the value of a state variable. In this way, since the effort and flow values of all bonds were obtained, the power of each bond can be computed. In summary, it means that the energy change for the propulsion system of the research vessel can be determined. The modeling results of hybrid mode, engine mode, motor mode, and charging mode are calculated for each mode in the same way as the previous calculation. However, since the load for each operation scenario is different in each mode, there are four modes (hybrid mode, engine mode, motor mode, and charging mode), and three operation scenarios (in-harbor navigation, transit to fishing ground navigation, and fishing operation navigation) exist. So, there are a total of 12 cases. The results of modeling in the Bond graph for hybrid mode, engine mode, motor mode, and charging mode are shown in Figures 7–10, respectively.

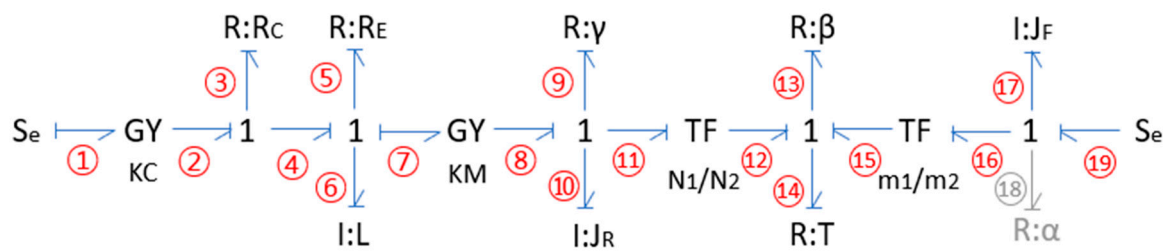


Figure 7. Bond graph modeling of hybrid mode.

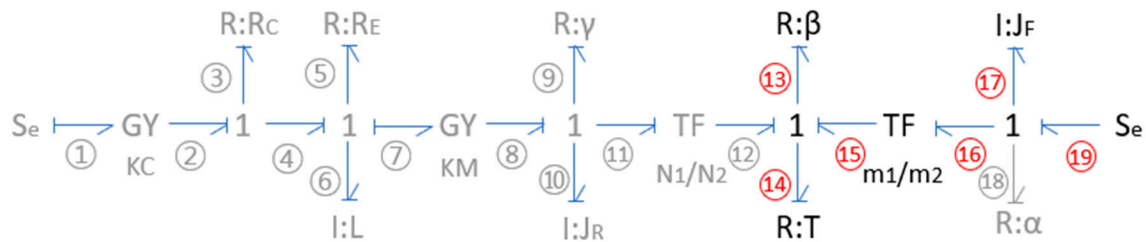


Figure 8. Bond graph modeling of engine mode.

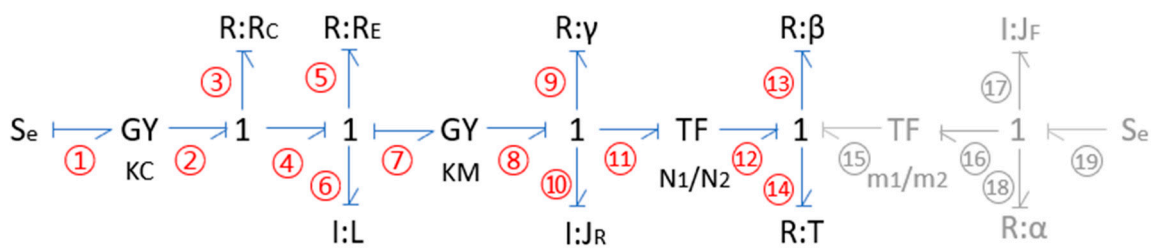


Figure 9. Bond graph modeling of motor mode.

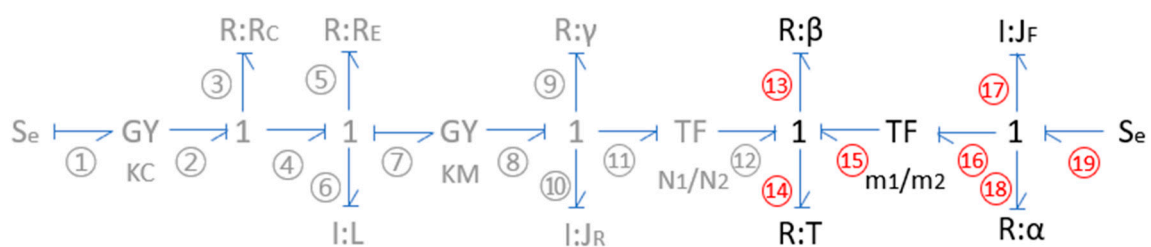


Figure 10. Bond graph modeling of charging mode.

## 6. Validation of Calculations

Next, the previous Bond graph modeling calculation result is verified. The verification method is determined by using the commercial software “20-sim 5.0” to model the same and comparing the value of the state variable [28]. However, it is essential to emphasize the difference between this study and commercial software before calculation verification. The commercial program only provides an environment for modeling by combining the concept of the Section 2. Bond graph and the elements introduced in the main contents but does not create the scheme of Figure 5 or provide modeling such as in Figure 6. In addition, the commercial program can be used universally, but it does not provide detailed analysis results for the propulsion system of the hybrid propulsion ship. Therefore, in this study, the performance estimation and energy flow can be calculated using the Bond graph modeling results for use in the initial design. The meaning of this study compared to the commercial program will be explained again in the results analysis. The following, Figure 11, shows the results of modeling hybrid modes using “20-sim 5.0” among the four modes.

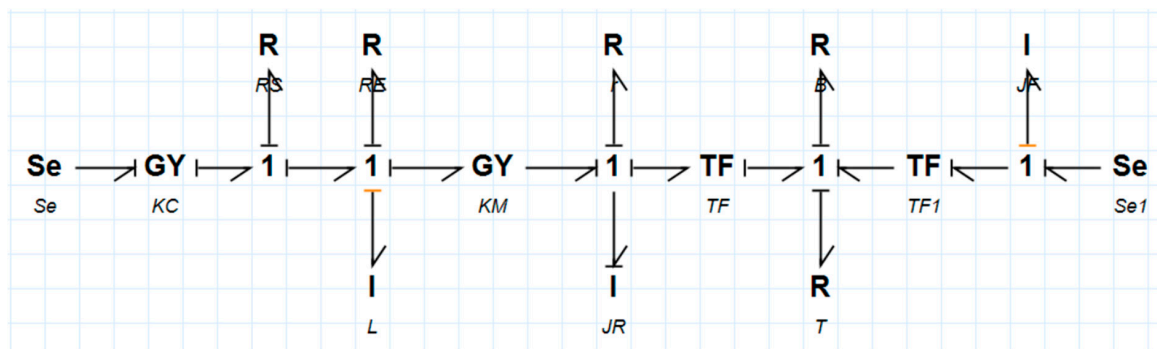


Figure 11. Bond graph modeling of hybrid mode by 20-sim 5.0.

In the case of using hybrid mode when moving to the fishing ground, the results of the study using the state variable value calculated through “20-sim 5.0” and the simultaneous ordinary differential equation derived through the energy flow calculation introduced in Section 5 (using the SciPy package(version 1.11.4) implemented by the Runge–Kutta 4th order method [29,30]) are compared as Figure 12.

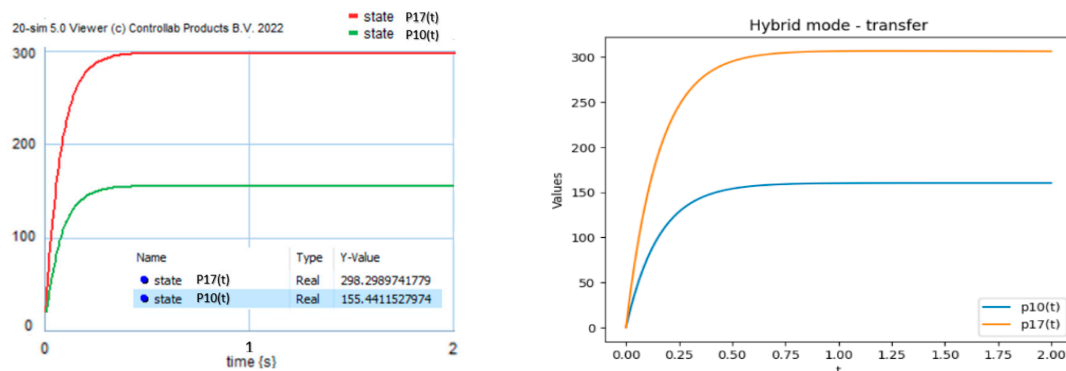


Figure 12. Result of 20-sim 5.0 (left) and study for Bond graph modeling (right).

The state variable corresponds to the variable bond 17( $p_{17}$ ) and the variable bond 10( $p_{10}$ ), and the physical meaning represents the energy stored in the rotational inertia of the engine flywheel and rotational inertia of the motor rotor, respectively. As a result of “20-sim 5.0”, bond 17( $p_{17}$ ) is [298.3] and bond 10( $p_{10}$ ) is [155.4], and the results of this study calculation using Bond graph modeling were found to be bond 17( $p_{17}$ ) as [306.4] and bond 10( $p_{10}$ ) as [160.3], respectively. For hybrid mode, engine mode, motor mode, and charging mode, the load conditions of each operation scenario (in-port operation, transit to fishing grounds, and fishing operation) are substituted and the results of this study are compared as follows. Table 7 shows that the average error for all 12 cases is around 2.8%. The reason for these differences is difficult to precisely ascertain due to the unknown solver of the commercial program. However, it is estimated to be attributed to differences in the solver used for solving ordinary differential equations.

Table 7. Comparison of “20-sim 5.0” and study result.

Mode	Operation	Energy Variable No.	20-sim	Study Result	Error (%)
Hybrid	in port	$p_{10}$	201.8	208.2	3.2%
	transfer	$p_{10}$	155.4	160.3	3.2%
	working	$p_{10}$	162.5	167.6	3.1%
	in port	$p_{17}$	387.3	398.2	2.8%
	transfer	$p_{17}$	298.3	306.4	2.7%
	working	$p_{17}$	311.8	320.3	2.7%

Table 7. Cont.

Mode	Operation	Energy Variable No.	20-sim	Study Result	Error (%)
Engine	in port	$p_{17}$	315.4	324.9	3.0%
	transfer	$p_{17}$	242.9	250.3	3.0%
	working	$p_{17}$	253.9	261.6	3.0%
Motor	in port	$p_{10}$	37.5	38.6	2.9%
	transfer	$p_{10}$	28.9	29.8	3.1%
	working	$p_{10}$	30.2	31.1	3.0%
Charging	in port	$p_{17}$	207.8	211.9	2.0%
	transfer	$p_{17}$	173.6	177.4	2.2%
Average	working	$p_{17}$	179.2	183.0	2.1%
					2.8%

## 7. Formalization of the Optimization Problem

In this study, the Bond graph modeling of a hybrid propulsion system is used to propose that it can be used in the initial design. To this end, it is necessary to set the objective function and related design variables with the aim of improving the performance of the ship. First of all, the objective function aimed to evaluate the overall voyages by integrating three distinct operational scenarios as the voyages scenarios of the research vessel are divided into “in-port navigation”, “transit between operation sites”, and “operation at site”. To achieve this, the value that can determine the performance in each operational scenario and the proportion (weighing factor) of the corresponding operational scenario in the total voyages were multiplied. In addition, in order to evaluate the overall voyages, the objective function was set to be maximized by summing up the values of each operational scenario. At this time, the value that can determine the performance in each operational scenario was set as the ratio of the required energy for propulsion to the energy input from the bond on the engine (or motor, or a combination of both) side in each operational scenario. This is expressed as an equation in the object function in Table 8.

Table 8. Formulation of optimization.

<b>&lt;Object Function&gt;</b>	
$F(x) = \max \left[ a * f_{port}(x_1, x_4) + b * f_{transfer}(x_2, x_4) + c * f_{working}(x_3, x_4) \right]$ $= \max \left[ a * f_{port}(T_{port}, TF) + b * f_{transfer}(T_{transfer}, TF) + c * f_{working}(T_{working}, TF) \right]$	
$x_1 (T_{port})$ : Power Consumption during In-port Navigation $x_2 (T_{transfer})$ : Power Consumption during Transit between Operation Sites $x_3 (T_{working})$ : Power Consumption during Operation at Site $x_4 (TF)$ : Reduction ratio $a$ : Weighted by Intra-port Navigation Time (In-port Navigation Time/Total Voyage Time) $b$ : Weighted by Transit to Operation Site Time (Transit to Operation Site Time/Total Voyage Time) $c$ : Weighted by Operation at Site Time (Operation at Site Time/Total Voyage Time) $f_{port}$ : Ratio of energy demanded during In-port Navigation to the energy input in the bond of the engine $f_{transfer}$ : Ratio of energy demanded during Transit to Operation Site to the energy input in the bond of the “engine + motor” $f_{working}$ : Ratio of energy demanded during Operation at Site to the energy input in the bond of the engine	
<b>&lt;Constraints&gt;</b>	
1. $(x_1 + Load_{charging}) < Engine\ Power / rps^2$ ..... physical conditions 2. $x_2 < (Engine\ Power + Motor\ Power) / rps^2$ ..... physical conditions 3. $x_3 < Engine\ Power / rps^2$ ..... physical conditions 4. $1 < x_4 < 5.91$ ..... system characteristics 5. $Engine\ Power < [a * x_1 + b * x_2 + c * x_3]$ ..... system characteristics	

The optimization variables for the above objective function were set to four types: “Reduction ratio”, “Power consumption during in-port navigation”, “Power consumption during transit to operation site”, and “Power consumption during operation at site”. When the engine and motor variables are set as optimization variables, there are many input variables for engine and motor specifications in the process of calculating the Bond graph, so if the variables of a specific part are optimized, it means that the engine and motor must be manufactured separately rather than off-the-shelf products. This is due to the lack of practicality, so in this study, a reduction gear was set as an optimization target. This is because the reduction gear is not only applied independently when calculating the Bond graph but also can effectively change the performance because it is at the contact point of all power transmission.

In addition, the design values of power consumption for each operational scenario are fixedly applied to the research target vessels under development (conducted by the MOF, energy-efficient and environment-friendly fishing vessel development research project, ‘21~25’). However, small fishing vessels have various operating patterns depending on the type of fish the vessels target and the maritime area. Therefore, in order to apply it practically to various ships, the optimized power consumption should be obtained by considering the operating time of each operational scenario. Therefore, the power consumption for each of the three operations—“power consumption during in-port navigation”, “power consumption during transit to operation site”, and “power consumption during operation at site”—were set as design variables for the optimization problem.

In summary, the core of this research formulation is to find the optimal power consumption for each operational scenario that can achieve maximum performance and the optimized reduction ratio when the operational scenario (in-port, transit to operation site, and operation at site) is determined according to type of fish the vessel target and maritime area.

Next, the constraints were set so that they did not violate physical conditions and system characteristics. First of all, the physical conditions are as follows. 1. During in-port navigation, the engine output is expected to exceed the sum of power consumption during in-port navigation and the charging load since the battery is charged during this state. 2. Since hybrid mode is used when moving to the operation site, the sum of engine and motor output will be greater than the power consumption during transit to the operation site. 3. Since only the engine is used during operation on the fishing ground, the engine output will be greater than the power consumption during operation in the working site.

Constraints according to the characteristics of the system are as follows. 4. In vessels, since the torque is increased and rotation speed is reduced through the reduction gear (to improve thrust and reduce cavitation), the reduction ratio will be greater than 1. Simultaneously, the reduction ratio should not exceed the maximum value for the reduction gear used in small vessels (up to a maximum of 5.91 for the tonnage of the specific vessel). 5. Since the entire voyage is evaluated, the representative value of the voyage is set to the sum of the product of the power consumption for each operational scenario and the ratio of usage time for each operational scenario (operational time for each scenario/total voyage time). This value is set to be greater than the engine output (if it is less than the engine output, it means the vessel can operate solely with the engine, rendering the hybrid mode unnecessary, indicating a mismatch with the system characteristics, and hence, setting a constraint). The above constraints are summarized as shown in Table 8 above.

## 8. Derivation of the Optimal Solution

The differential evolution method was employed for the optimization problem [31]. In order to find the optimal solution, it is necessary to be able to consider both physical constraints and constraints during Bond graph calculations. Moreover, in order to derive the global optimum, the differential evolution method was used because it had to be possible to find the optimal value by changing the initial value. Next is the evaluation criterion for convergence. The analysis result was judged to converge when the two criteria

were satisfied. The first was judged to show the same result while increasing the population size in consideration of repetitive reproducibility. Second, the convergence was evaluated by monitoring how the optimal value responded to changes in inputs. As the purpose of this study is to use it for the initial design stage in consideration of the characteristics of different types of fish that vessels target and maritime areas, the input value is the usage time for each regional operational scenario. Therefore, the usage time for each regional operational scenario was investigated based on the interview with fishermen, and the results are shown in Table 9. In other words, it was applied as a criterion for determining whether the constraints to be activated change when the time value of the regional operational scenario is changed as shown in Table 9. This is because the objective function or constraint is inappropriate if only the same constraint operates according to the change in the input value. To summarize the contents so far, the problem can be expressed as shown in Figure 13.

**Table 9.** Operation scenario (A: operation time in port, B: operation time during transfer, C: operation time at working on site).

Description	Total Time (T) [h]	In Port		Transfer		Working	
		Time (A) [h]	Non-Dimensional (A/T)	Time (B) [h]	Non-Dimensional (B/T)	Time (C) [h]	Non-Dimensional (C/T)
West Sea	9.00	0.25	0.03	3.25	0.36	5.50	0.61
South Sea	13.75	1.25	0.09	3.50	0.25	9.00	0.65
East Sea	16.4	1.5	0.1	3.9	0.24	11	0.67

Accordingly, as a result of optimization, the “Reduction ratio”, “Power consumption during in-port navigation”, “Power consumption during transit to operation site”, and “Power consumption during operation at site” for each operation scenario change in each region are shown in Table 10.

**Table 10.** Result of optimization for load and reduction ratio.

Description	Optimum Load [N·m/(rad/s)]			Reduction Ratio
	In Port	Transfer from Port to Fishing Ground	Working (Fishing)	
West Sea	194.6	196.4	204.0	3.72
South Sea	209.9	196.4	224.2	4.09
East Sea	206.6	196.4	219.7	4.01

Table 10 corresponds to the effort value of bond 14 on the Bond graph and is converted into a power unit by multiplying the flow value of bond 14 as shown in Table 11. Bond 14 flow can be calculated according to Equation (14).

**Table 11.** Result of optimization for load and reduction ratio(convert to KW).

Description	Optimum Load [kW]			Reduction Ratio
	In Port	Transfer from Port to Fishing Ground	Working (Fishing)	
West Sea	125.9	106.9	167.4	3.72
South Sea	123.6	117.4	184.0	4.09
East Sea	124.1	115.1	180.3	4.01

## 9. Analysis of Results

In order to analyze the trend for the optimization result, it is necessary to visualize the result. However, since there are four optimization design variables, they cannot be expressed at once. Therefore, it was visualized by dividing the contour graph into six sections so that the objective function value for the two optimization design variables ( $x, y$ ) became  $z$ , and the results are shown in Figures 13–15. The results include the values of the objective function corresponding to changes in two optimization design variables, along with the optimal values of each design variable and the regions of the constraints. In each figure, “ $TF$ ” is the reduction ratio, and “ $T$ ” denotes the power [ $N \cdot m / (rad/s)$ ] consumed as the “ $T$  value” in Figure 6. “ $T_{c\_pt}$ ” and “ $T_{e\_wk}$ ” are the same “ $T$  value” in Figure 6 when calculating the Bond graph, but “ $T$ ”, “ $T_{c\_pt}$ ”, and “ $T_{e\_wk}$ ” mean the power consumed during transit, power consumption during in-port navigation, and power consumption during operation in site, respectively.

Let us first look at the general trend and analyze the differences according to the regional operational scenarios. The general trend is as follows.

The graphs ① to ③ of Figures 13–15 show the relationship between the reduction ratio ( $TF$ ) and power consumption during in-port navigation ( $T_{c\_pt}$ ), transit power consumption ( $T$ ), and operation in site power consumption ( $T_{e\_wk}$ ). It can be seen that the objective function tends to be maximized when the reduction ratio ( $TF$ ) is maximized while minimizing each power consumption. This trend is consistent with the general trend of increasing the propulsion efficiency by increasing the reduction ratio while minimizing the power consumption for operation. In addition, when looking through the area of the constraints displayed in white, the transit power consumption ( $T$ ) is not sensitive to the constraints, but the power consumption during in-port navigation ( $T_{c\_pt}$ ) and operation in site ( $T_{e\_wk}$ ) are affected by the constraints. In particular, it can be seen that the optimal point for power consumption during in-port navigation ( $T_{c\_pt}$ ) is located near the constraint region and is most affected by constraints. It can be said that the efficiency of operation is affected in the entire voyage according to the hybrid propulsion, which also serves the energy charged in charging mode within the port for movement to the fishing ground, concurrently employing the motor.

The graphs ④ to ⑥ of Figures 13–15 are the results of analyzing the effects on power consumption during intra-port navigation ( $T_{c\_pt}$ ), transit power consumption ( $T$ ), and operation power consumption ( $T_{e\_wk}$ ). When evaluated by the slope of the contour lines, it can be seen that the slope is sharp in the relationship between operation power consumption ( $T_{e\_wk}$ ) and transit power consumption ( $T$ ), and the impact of the transit power consumption ( $T$ ) is large. Second, the power consumption during in-port navigation ( $T_{c\_pt}$ ) and transit power consumption ( $T$ ) have similar effects when looking at the slope of the graph. Third, looking at the relationship between power consumption during in-port navigation ( $T_{c\_pt}$ ) and operation in site power consumption ( $T_{e\_wk}$ ), it can be seen that the slope of the contour lines is gentle, and the influence of power consumption during in-port navigation ( $T_{c\_pt}$ ) has a significant impact.

In addition, the difference according to the operational scenario of each maritime region is analyzed as follows. The contour lines for each sea area have similar results. However, in the case of the West Sea, the operating distance and operating time are short depending on the sea boundary with China. Therefore, the preparation time for departure from the port is short, and looking at the fifth graph in Figure 13 (West Sea), it can be seen that the slope of the contour lines of the power consumption during in-port navigation ( $T_{c\_pt}$ ) and transit power consumption ( $T$ ) is gentle compared to other maritime regions. In other words, in this hybrid propulsion method, how much battery is charged in the port is an important part of efficient operation for the entire voyage.

In addition, it was observed that the optimal reduction ratio was derived differently depending on the operation scenario of each maritime region. It is judged that this can contribute to the performance improvement of the ship by reviewing the operation time during the initial design stage and determining the optimal reduction ratio.

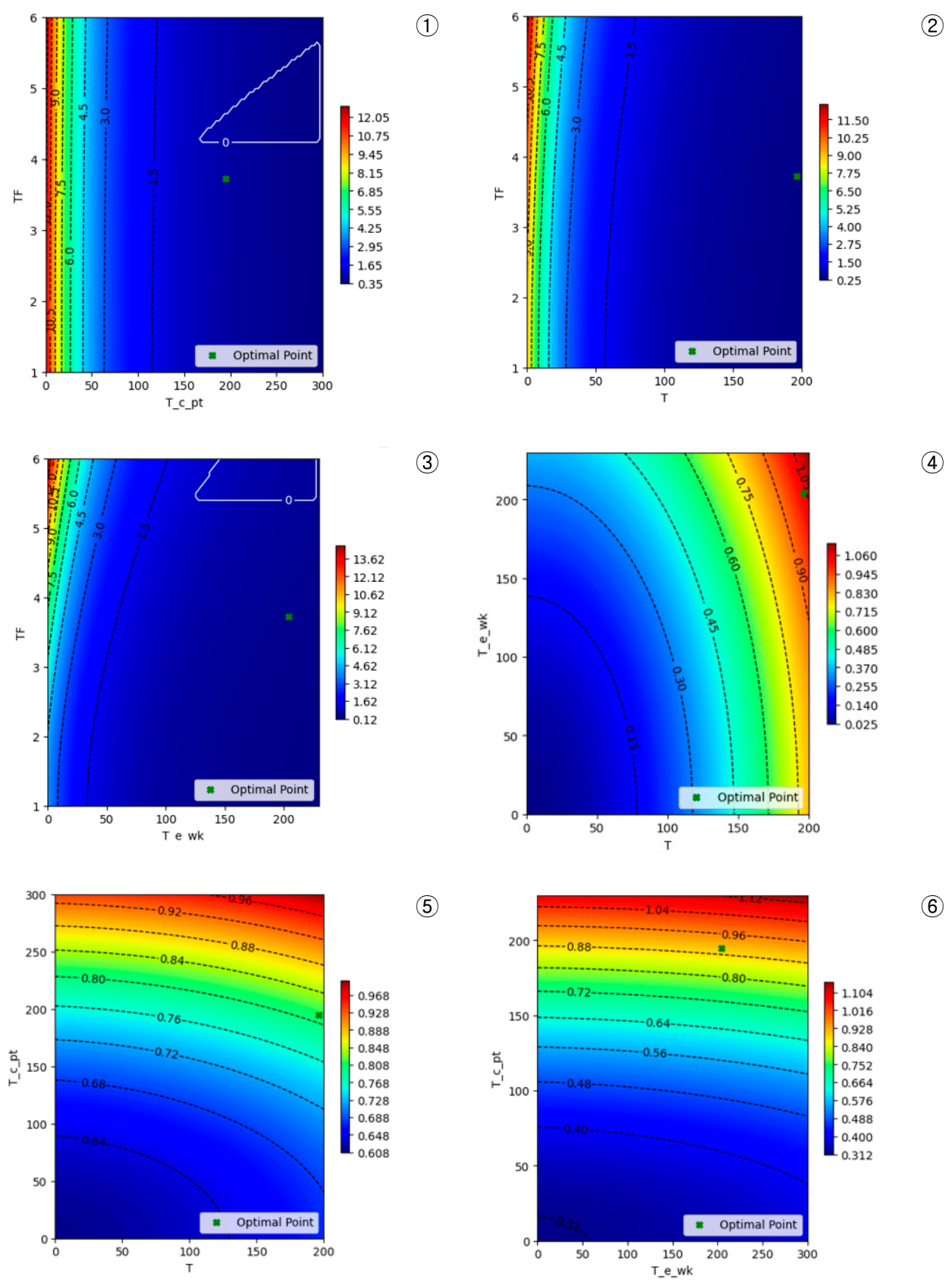


Figure 13. Contour of optimization for West Sea.

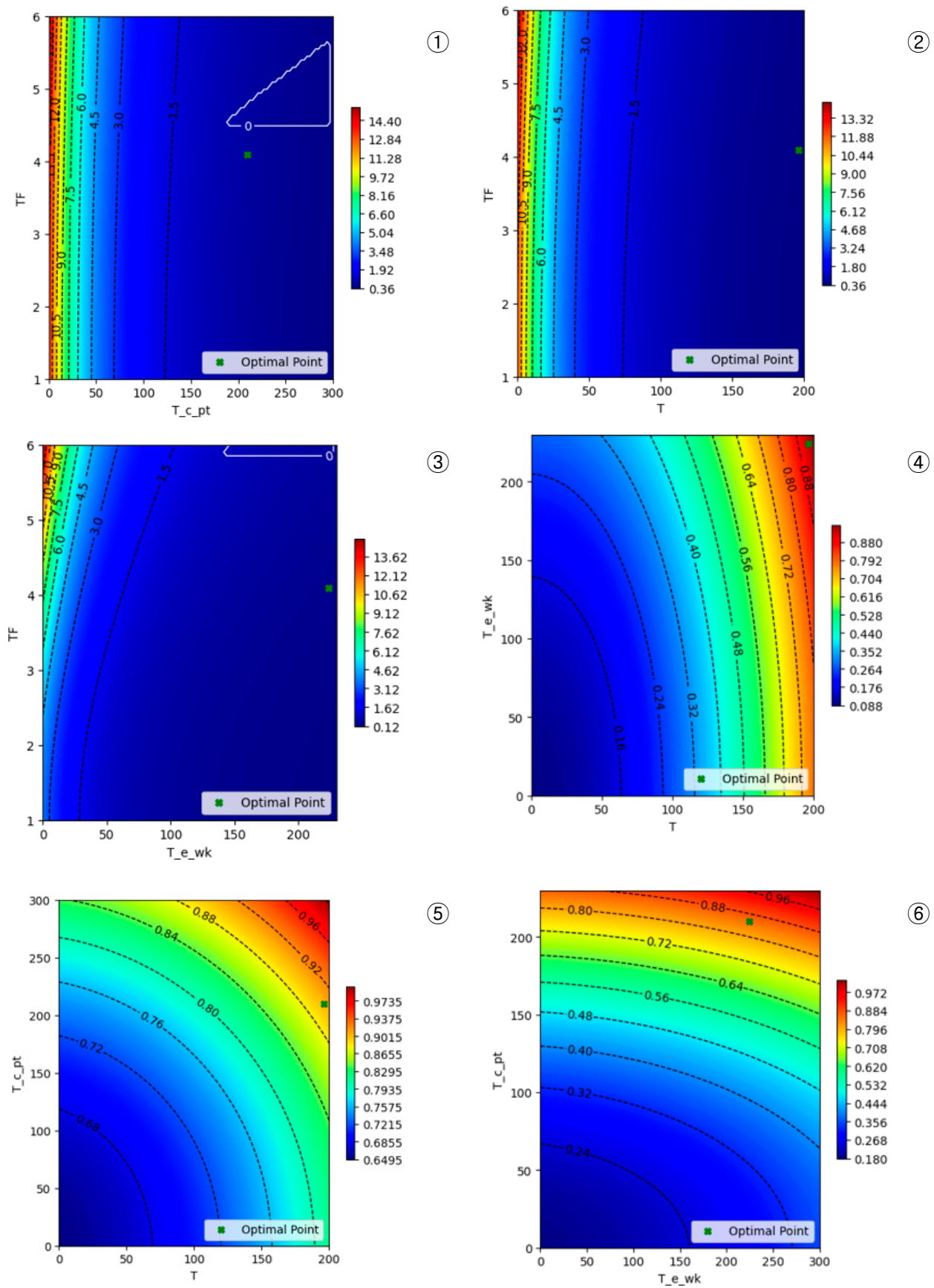


Figure 14. Contour of optimization for South Sea.

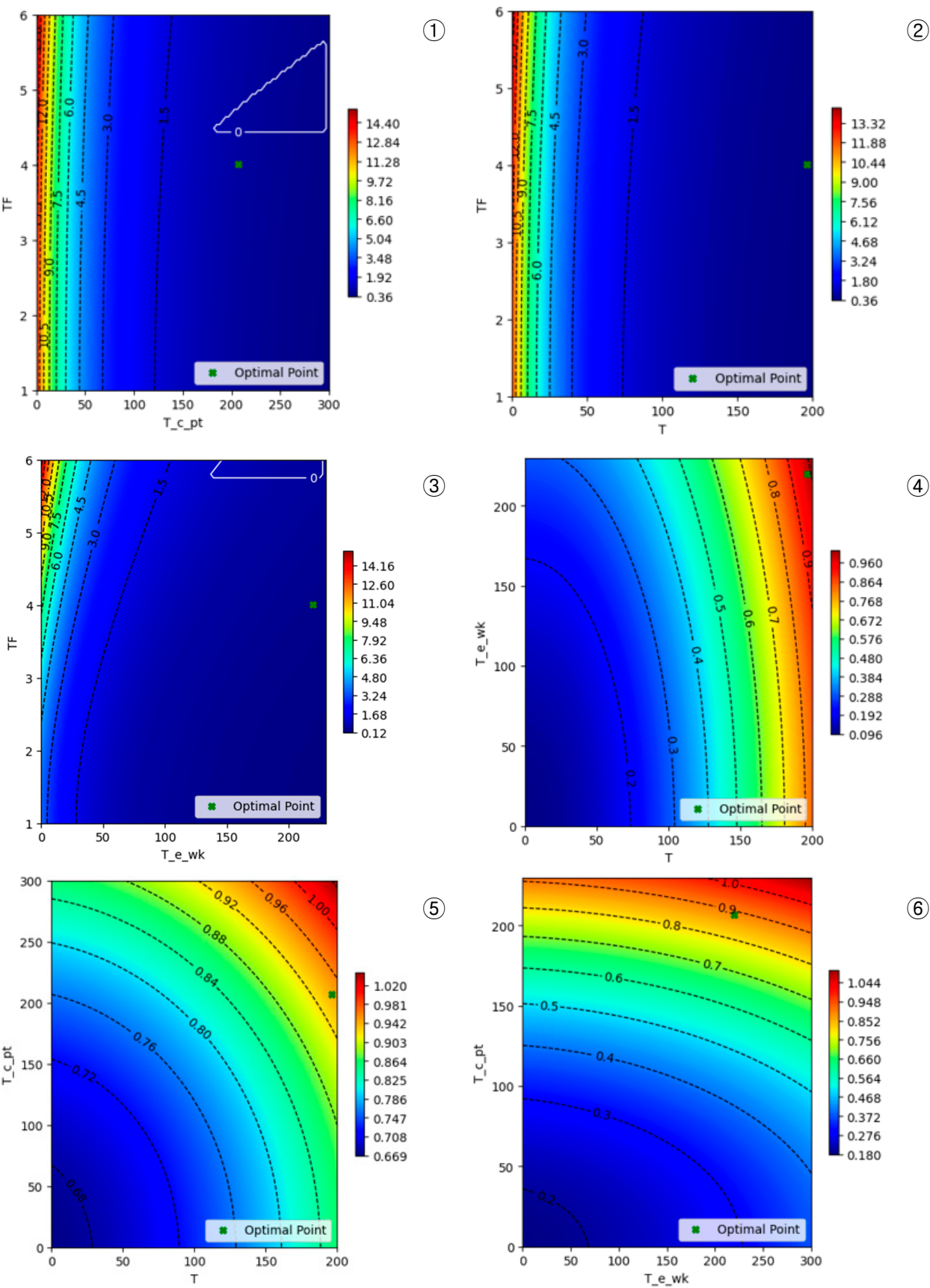


Figure 15. Contour of optimization for East Sea.

## 10. Conclusions

The supply of hybrid propulsion (diesel and electric complex propulsion) ships is expected to increase in accordance with the demand for eco-friendly ships. This is because small ships have a limitation of space to install an LNG propulsion system, etc., and the risk of accidents at sea is increased when the battery is exhausted to apply only battery propulsion.

However, the design of most small ships, including fishing vessel, is generally completed in a way that slightly changes the design by reflecting the requirements of the order based on the design information of reference ship. Also, it is very rare to have an R&D base. Therefore, if hybrid propulsion ships such as the research target ship (MOF, energy-saving and eco-friendly fishing boat development research project, '21~25') are distributed, it is expected that there will be difficulties in changing the design because there is no reference ship and R&D base.

Therefore, in the results of this study, when the ratio of the usage time for each operation scenario per vessel is input, the optimized reduction ratios and operation point (power consumption) can be derived. Since the reduction ratio is a key design variable of the reduction gear and is at the contact point (Node) when all power is transmitted, an efficient performance change can be expected while minimizing design changes compared to modifying other factors in the propulsion system.

In addition, considering the design conditions of small ships with limited scale and R&D capabilities, it is expected to be practical because the performance of the ship can be changed in consideration of the operating characteristics of each maritime regions and catching methods for target fish with minimal design change in the reference ship. In addition, this study is expected to be useful in contributing to the widespread adoption of hybrid propulsion ships because it can recommend efficient operational points for the entire voyage to users by presenting the required power for each operation scenario.

In summary, the transition to eco-friendly ships, such as small vessels like fishing boats, is expected to involve the application of hybrid electric propulsion systems. The studies related to hybrid electric propulsion vessels are currently underway to develop models optimized for specific tonnages and vessel types. However, utilizing the findings of this study could maximize the utility of eco-friendly vessels by enabling more efficient navigation, considering the characteristics of various maritime regions and vessel types. Nevertheless, due to the lack of comprehensive data on equipment specifications for various model such as engines and motors, this study was limited to optimizing specifications for reduction gear only. It is anticipated that future studies will be able to expand optimization targets to include engines, motors, and other equipment if more information becomes available. This would enable subsequent studies to select various equipment.

**Author Contributions:** The first author S.-W.M. led the planning, model development, and interpretation of the research. The corresponding W.-S.R. supervised the optimization algorithm and the project based on the model development. All authors discussed the results and exchanged opinions regarding the manuscript. The K.-P.P. proposed the conceptual methodology of the Bond graph. All authors have read and agreed to the published version of the manuscript.

**Funding:** This research received no external funding.

**Institutional Review Board Statement:** Not applicable.

**Informed Consent Statement:** Not applicable.

**Data Availability Statement:** The data in this study are available from the corresponding authors on request.

**Acknowledgments:** This work was supported by research fund of Chungnam National University.

**Conflicts of Interest:** The authors declare no competing financial interests.

## Abbreviations

$e_i$	Effort (power variable)
$f_i$	Flow (power variable)
GY	Convert element (convert effort to flow, flow to effort)
I, C	Storage element
$p_i$	Momentum (energy variable)
$q_i$	Displacement (energy variable)
R	Dissipator element
$s_e, s_f$	Source element
TF	Transform element (transform effort to effort, flow to flow)
0 Junction	Distribution element (all effort is distributed as same)
1 Junction	Distribution element (all flow is distributed as same)

## References

- Ahn, J. A Study on Improvement for Greenship Certification Scheme to Achieve Net-Zero. *J. Soc. Nav. Archit. Korea* **2022**, *59*, 372–384. [CrossRef]
- Park, J.; Lee, K.-S.; Lee, K.; Kim, J.; Choi, J.; Lee, M. A Study on the Performance Evaluation of An Electrospray Scrubber for Simultaneous Removal of PM/NOx/Sox; Summer conference paper collection; The Society of Air-Conditioning and Refrigerating Engineers of Korea: Seoul, Republic of Korea, 2022; pp. 356–357.
- Yeo, I.; Park, C.G. Study on Performance Evaluation of SOx-NOx Wet Scrubber Wastewater Treatment System in Ship; Winter conference paper collection; The KSFM Journal of Fluid Machinery: Jeju Island, Republic of Korea, 2022.
- Choia, M.-S. A Study on Prospects for the Introduction of LNG Fueled Ships. *J. Int. Trade Commer.* **2023**, *19*, 329–333.
- Kim, J.-S.; Kim, D.-Y.; Kim, Y.-T. A Fundamental Study on Boil-Off Gas Re-Liquefaction Systems for LNG-Fueled Ship; Winter Conference Paper Collection; The KSFM Journal of Fluid Machinery: Jeju Island, Republic of Korea, 2022.
- Lee, W.-J.; Kim, J.-S.; Yeo, S.-J.; Noh, J.-H.; Kim, T.-G.; Lee, J.-W.; Lee, J.-U.; Jeon, H.-M. Demand analysis and environmental assessment for LPG fuelled ships. In Proceedings of the Spring Academic Conference, Online, 24–25 June 2021.
- Lee, C.; Oh, J.; You, B.; Kim, D. A Numerical Study on Reduction of Nitrogen Oxide and Black Carbon According to Combustion Parameters of Marine Engine with DME fuels. In Proceedings of the Spring Academic Conference, Online, 25–26 June 2020.
- Jee, J.-H. A Study on Risk Assessment using What-If Method for Ammonia Fueled Ship. *J. Fishries Mar. Sci. Educ.* **2023**, *35*, 783–795. [CrossRef]
- Hwang, J.; Jeon, H.; Hur, J.; Yoon, K.; Kim, J. A Study on eco-friendly ship propulsion system applicable to fishing vessels. In Proceedings of the Fall Academic Conference, Pusan, Republic of Korea, 24–25 November 2022.
- Number of Fishing Vessel by Tonnage and Type of Construction Material. Available online: [https://kosis.kr/statHtml/statHtml.do?orgId=146&tblId=DT\\_MLTM\\_5002762&vw\\_cd=MT\\_ZTITLE&list\\_id=K2\\_1&seqNo=&lang\\_mode=ko&language=kor&obj\\_var\\_id=&itm\\_id=&conn\\_path=MT\\_ZTITLE/](https://kosis.kr/statHtml/statHtml.do?orgId=146&tblId=DT_MLTM_5002762&vw_cd=MT_ZTITLE&list_id=K2_1&seqNo=&lang_mode=ko&language=kor&obj_var_id=&itm_id=&conn_path=MT_ZTITLE/) (accessed on 2 September 2023).
- Fisheries ACT, [Enforcement Date 12. Jan, 2023.] [Act No.18755, 11. January 2022, Whole Amendment], Article 58 (Restrictions on Bottoms of Fishing Vessels). Available online: <https://www.law.go.kr/%20engLsSc.do?menuId=1&subMenuId=21&tabMenuId%20=117&query=%EC%88%98%EC%25%2082%B0%EC%97%85%EB%B2%95#> (accessed on 2 September 2023).
- Enforcement Decree of Fisheries ACT. [Enforcement Date 12 January 2024.] [Act No.34119, 9. March, 2024., Partial Amendment], Article 37. Available online: <https://www.law.go.kr/lsSc.do?section=&menuId=1&subMenuId=15&tabMenuId=81&eventGubun=060101&query=%EC%88%98%EC%82%B0%EC%97%85%EB%B2%95#37:0> (accessed on 2 September 2023).
- Enforcement Decree of Fisheries ACT. [Enforcement Date 12. Jan, 2024.] [Act No.34119, 9. March, 2024., Partial Amendment], Article 37, Appendix 6. Available online: <https://www.law.go.kr/sBylInfoPLinkR.do?lsiSeq=258361&lsNm=%EC%88%98%EC%82%B0%EC%97%85%EB%B2%95+%EC%8B%9C%ED%96%89%EB%A0%B9&bylNo=0006&bylBrNo=00&bylCls=BE&bylEfYd=20240112&bylEfYdYn=Y/> (accessed on 2 September 2023).
- Bae, C.-S.; Yang, W.-J. Analysis of the Importance of Eco-friendly Ship Dissemination Policy using the Analytic Hierarchy Process. *J. Korean Soc. Mar. Environ. Saf. Res. Pap.* **2022**, *28*, 117–124. [CrossRef]
- Kang, C.E.; Baek, C.H.; Kim, S.H.; Lee, C.J. A Study of the Development Safety Criteria for Hybrid Electrical Propulsion Fishing Boats. *J. Korean Soc. Mar. Environ. Saf. Res. Pap.* **2023**, *29*, 207–214.
- You, Y.-J.; Park, H.-R. Development of a framework to estimate the EEOI of a ship considering the hydrodynamic characteristics and engine mode. *J. Soc. Nav. Archit. Korea* **2018**, *55*, 457–465. [CrossRef]
- Ghimire, P.; Reddy, N.P.; Zadeh, M.K.; Pedersen, E.; Thorstensen, J. Dynamic Modeling and Real-Time Simulation of a Ship Hybrid Power System Using a Mixed-Modeling Approach. In Proceedings of the 2020 IEEE Transportation Electrification Conference & Expo (ITEC), Chicago, IL, USA, 23–26 June 2020. originally scheduled.
- Ghimire, P.; Zadeh, M.; Pedersen, E.; Thorstensen, J. Dynamic Modeling, Simulation, and Testing of a Marine DC Hybrid Power System. *IEEE Trans. Transp. Electrif.* **2021**, *7*, 905–919. [CrossRef]
- Moon, S.-W.; Ruy, W.-S. A Study on the Modeling of Ship Energy System Using Bond Graph. *J. Soc. Nav. Archit. Korea* **2024**, *61*, 19–28. [CrossRef]

20. National Institute of Fisheries Science. Available online: <https://www.nifs.go.kr/> (accessed on 2 September 2023).
21. Jung, S.-J.; Kim, I.-O.; Park, C.-D.; Kim, S.-H.; Jeong, G.-C. *Illustration of Korea Fishing Vessels*; National Fisheries Research and Development Institute: Quezon City, Philippines, 2018.
22. Bond Graph.com. About Bond Graph. Available online: <https://www.scribd.com/document/48821925/Samantaray-2001-www-bondgraphs-com-about/> (accessed on 2 September 2023).
23. Merzouki, R.; Samantaray, A.K.; Pathak, P.M.; Bouamama, B.O. *Intelligent Mechatronic Systems Modeling, Control and Diagnosis*; Springer: Berlin/Heidelberg, Germany, 2013.
24. Borutzky, W. *Bond Graph Methodology Development and Analysis of Multidisciplinary Dynamic System Models*; Springer: Berlin/Heidelberg, Germany, 2010.
25. Kim, J.-S.; Park, J.-S. Basic concepts of Bond graph modeling techniques and its applications. *J. Korean Soc. Mech. Eng.* **1993**, *33*, 22–32.
26. Pedersen, T.A. Bond Graph Modeling of MarinePower Systems. Ph.D. Thesis, Norwegian University of Science and Technology, Trondheim, Norway, 2009.
27. Ayala-Jaimes, G.; Gonzalez-Avalos, G. MOSFET Modelling for A Three-Level Inverter Circuit: A Hybrid Bond graph Approach. In Proceedings of the 48th Annual Conference of the IEEE Industrial Electronics Society, Brussels, Belgium, 17–20 October 2022.
28. 20-sim 5.0. Available online: <https://www.20sim.com/> (accessed on 2 September 2023).
29. Runge-Kutta Method. Available online: [https://ko.wikipedia.org/wiki/%EB%A3%BD%EA%B2%8C-%EC%BF%A0%ED%83%80\\_%EB%B0%A9%EB%B2%95/](https://ko.wikipedia.org/wiki/%EB%A3%BD%EA%B2%8C-%EC%BF%A0%ED%83%80_%EB%B0%A9%EB%B2%95/) (accessed on 2 September 2023).
30. SciPy Library. Available online: <https://docs.scipy.org/doc/scipy/reference/generated/scipy.optimize.minimize.html/> (accessed on 2 September 2023).
31. Differential Evolution. Available online: [https://docs.scipy.org/doc/scipy/reference/generated/scipy.optimize.differential\\_evolution.html/](https://docs.scipy.org/doc/scipy/reference/generated/scipy.optimize.differential_evolution.html/) (accessed on 2 September 2023).

**Disclaimer/Publisher’s Note:** The statements, opinions and data contained in all publications are solely those of the individual author(s) and contributor(s) and not of MDPI and/or the editor(s). MDPI and/or the editor(s) disclaim responsibility for any injury to people or property resulting from any ideas, methods, instructions or products referred to in the content.